

Elastic neutron scattering at 96 MeV from  $^{12}\text{C}$  and  $^{208}\text{Pb}$ 

J. Klug,<sup>1</sup> J. Blomgren,<sup>1,\*</sup> A. Ataç,<sup>1</sup> B. Bergenwall,<sup>1</sup> A. Hildebrand,<sup>1</sup> C. Johansson,<sup>1</sup> P. Mermod,<sup>1</sup> L. Nilsson,<sup>1</sup> S. Pomp,<sup>1</sup> U. Tippawan,<sup>1</sup> K. Elmgren,<sup>2</sup> N. Olsson,<sup>2</sup> O. Jonsson,<sup>3</sup> A. V. Prokofiev,<sup>3</sup> P.-U. Renberg,<sup>3</sup> P. Nadel-Turonski,<sup>4</sup> S. Dangtip,<sup>5</sup> P. Phansuke,<sup>5</sup> M. Österlund,<sup>6</sup> C. Le Brun,<sup>7</sup> J. F. Lecolley,<sup>7</sup> F. R. Lecolley,<sup>7</sup> M. Louvel,<sup>7</sup> N. Marie-Noury,<sup>7</sup> C. Schweitzer,<sup>7</sup> Ph. Eudes,<sup>8</sup> F. Haddad,<sup>8</sup> C. Lebrun,<sup>8</sup> A. J. Koning,<sup>9</sup> E. Bauge,<sup>10</sup> J. P. Delaroche,<sup>10</sup> M. Girod,<sup>10</sup> X. Ledoux,<sup>10</sup> P. Romain,<sup>10</sup> D. G. Madland,<sup>11</sup> K. Amos,<sup>12</sup> P. K. Deb,<sup>12</sup> S. Karataglidis,<sup>12</sup> R. Crespo,<sup>13</sup> and A. M. Moro<sup>13</sup>

<sup>1</sup>*Department of Neutron Research, Uppsala University, Box 525, S-75120 Uppsala, Sweden*

<sup>2</sup>*Swedish Defence Research Agency (FOI), Stockholm, Sweden*

<sup>3</sup>*The Svedberg Laboratory, Uppsala University, Uppsala, Sweden*

<sup>4</sup>*Department of Radiation Sciences, Uppsala University, Uppsala, Sweden*

<sup>5</sup>*Department of Physics, Chiang Mai University, Chiang Mai, Thailand*

<sup>6</sup>*Department of Physics, University of Jönköping, Jönköping, Sweden*

<sup>7</sup>*LPC, ISMRA et Université de Caen, CNRS/IN2P3, Caen, France*

<sup>8</sup>*SUBATECH, Université de Nantes, CNRS/IN2P3, Nantes, France*

<sup>9</sup>*NRG, Petten, The Netherlands*

<sup>10</sup>*DPTA/SPN CEA, Bruyères-le-Châtel, France*

<sup>11</sup>*Theoretical Division, Los Alamos National Laboratory, Los Alamos, New Mexico 87545*

<sup>12</sup>*School of Physics, University of Melbourne, Victoria, Australia*

<sup>13</sup>*Departamento de Física, Instituto Superior Técnico, Lisboa, Portugal*

(Received 6 December 2002; published 25 March 2003)

A facility for detection of scattered neutrons in the energy interval 50–130 MeV, scattered nucleon detection assembly, has recently been installed at the 20–180 MeV neutron beam line of The Svedberg Laboratory, Uppsala. First results on elastic neutron scattering from  $^{12}\text{C}$  and  $^{208}\text{Pb}$  at 96 MeV incident neutron energy are presented. This experiment represents the highest neutron energy where the ground state has been resolved from the first excited state in neutron scattering. The results are compared with modern optical model predictions.

DOI: 10.1103/PhysRevC.67.031601

PACS number(s): 24.10.Ht, 25.40.Dn, 28.20.Cz

The interest in high-energy neutron data is rapidly growing, since a number of potential large-scale applications involving fast neutrons are under development, or at least have been identified. These applications primarily fall into three sectors: nuclear energy and waste, nuclear medicine, and effects on electronics.

For all these applications, an improved understanding of neutron interactions is needed for calculations of neutron transport and radiation effects. The nuclear data needed for this purpose come almost entirely from nuclear scattering and reaction model calculations, which all depend heavily on the optical model, which in turn is determined by elastic scattering and total cross section data.

The present work is part of the EU project HINDAS (high and intermediate energy nuclear data for accelerator-driven systems) [1], which has been designed to meet the demand for new nuclear data for feasibility assessments of accelerator-based transmutation techniques. It is, however, also relevant for various biomedical applications.

Neutron scattering data are also important for a fundamental understanding of the nucleon-nucleus interaction, in particular for determining the isovector term [2]. Coulomb repulsion of protons creates a neutron excess in all stable nuclei with  $A > 40$ . Incident protons and neutrons interact differently with this neutron excess. The crucial part in these

investigations has been neutron-nucleus elastic scattering data to complement the already existing proton-nucleus data.

Above 50 MeV neutron energy, there has been only one measurement on neutron elastic scattering with an energy resolution adequate for resolving individual nuclear states, an experiment at UC Davis at 65 MeV on a few nuclei [3]. In addition, a few measurements in the  $0^\circ$ – $20^\circ$  range are available, all with energy resolution of 20 MeV or more. This is, however, not crucial at such small angles because elastic scattering dominates heavily, but at larger angles such a resolution would make data very difficult to interpret.

The neutron beam facility at The Svedberg Laboratory, Uppsala, Sweden, has recently been described in detail [4], and therefore only a brief description is given here. The  $96 \pm 0.5$  MeV [1.2-MeV FWHM (full width at half maximum)] neutrons were produced by the  $^7\text{Li}(p,n)$  reaction by bombarding a  $427 \text{ mg/cm}^2$  disk of isotopically enriched (99.98%)  $^7\text{Li}$  with protons from the cyclotron. The low-energy tail of the source neutron spectrum was suppressed by time-of-flight techniques. After the target, the proton beam was bent into a well-shielded beam dump. A system of three collimators defined a 9-cm-diameter neutron beam at the scattering target.

Scattered neutrons were detected by the scattered nucleon detection assembly (SCANDAL) setup [4]. It consists of two identical systems, placed to cover  $10^\circ$ – $50^\circ$  and  $30^\circ$ – $70^\circ$ , respectively. The energy of the scattered neutron is determined by measuring the energy of proton recoils from a plas-

\*Corresponding author. Email address: jan.blomgren@tsl.uu.se

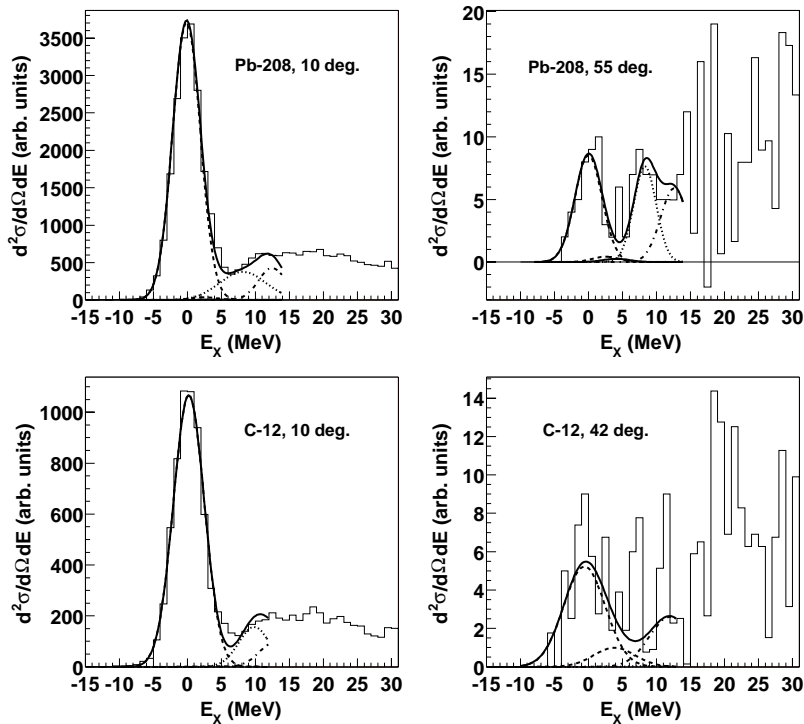


FIG. 1. Excitation energy spectra for elastic neutron scattering from  $^{12}\text{C}$  and  $^{208}\text{Pb}$  at 96 MeV incident neutron energy, together with Gaussians representing known excited states. See the text for details.

tic scintillator, and the angle is determined by tracking the recoil proton. In the present experiment, each arm consisted of a 2-mm-thick veto scintillator for fast charged-particle rejection, a 10-mm-thick neutron-to-proton converter scintillator, a 2-mm-thick plastic scintillator for triggering, two drift chambers for proton tracking, a 2-mm-thick  $\Delta E$  plastic scintillator which was also part of the trigger, and an array of CsI detectors for energy determination of recoil protons produced in the converter by neutron-proton ( $n$ - $p$ ) scattering. The trigger was provided by a coincidence of the two trigger scintillators, vetoed by the front scintillator. The total excitation energy resolution varies with CsI crystal, but is on average 3.7-MeV FWHM. The angular resolution is in the  $1.0^\circ$ – $1.3^\circ$  (rms) range.

Two targets were used, a carbon cylinder, 5 cm high and 5 cm in diameter, with a mass of 178 g and a natural isotopic composition (98.9%  $^{12}\text{C}$ ), and a radiogenic lead cylinder (88%  $^{208}\text{Pb}$ ), 6.3 cm high and 2.9 cm in diameter, with a mass of 444 g.

Excitation energy spectra are presented in Fig. 1. In these spectra, Gaussians representing known states are indicated. For  $^{12}\text{C}$ , the ground state ( $0^+$ ) and the two collective states at 4.4 MeV ( $2^+$ ) and 9.6 MeV ( $3^-$ ) are shown. In the case of  $^{208}\text{Pb}$ , the ground state ( $0^+$ ) and the two collective states at 2.6 MeV ( $3^-$ ) and 4.1 MeV ( $2^+$ ) are shown, as well as a Gaussian at 8.3 MeV representing a cluster of weak states. For both nuclei, a Gaussian at 12.6 MeV represents the opening of conversions due to  $^{12}\text{C}(n,p)$  reactions in the converter scintillator, i.e., an instrument background. As can be seen, in no case the population of excited states seriously affects the determination of the ground state cross section.

Angular distributions of elastic neutron scattering from  $^{12}\text{C}$  and  $^{208}\text{Pb}$  at 96 MeV incident neutron energy are presented in Fig. 2. The data are compared with phenomeno-

logical and microscopic optical model predictions in the upper and lower panels, respectively. The theoretical curves have all been folded with the experimental angular resolution to facilitate comparisons with data. The data by Salmon at 96 MeV [5] are also shown.

The angular distributions presented have been corrected for reaction losses and multiple scattering in the target. The contribution from isotopes other than  $^{208}\text{Pb}$  in the lead data has been corrected for, using cross section ratios calculated with the global potential by Koning and Delaroche [6]. The absolute normalization of the data has been obtained from knowledge of the total elastic cross section, which has been determined from the difference between the total cross section  $\sigma_T$  [7] and the reaction cross section  $\sigma_R$  [8,9]. This  $\sigma_T - \sigma_R$  method, which is expected to have an uncertainty of about 3%, has been used to normalize the  $^{12}\text{C}$  data. The present  $^{208}\text{Pb}(n,n)$  data have been normalized relative to the present  $^{12}\text{C}(n,n)$  data, knowing the relative neutron fluences, target masses, etc. The total elastic cross section of  $^{208}\text{Pb}$  has previously been determined with the  $\sigma_T - \sigma_R$  method. The accuracy of the present normalization has been tested by comparing the total elastic cross section ratio ( $^{208}\text{Pb}/^{12}\text{C}$ ) obtained with the  $\sigma_T - \sigma_R$  method above, and with the ratio determination of the present experiment, the latter being insensitive to the absolute scale. These two values differ by about 3%, i.e., they are in agreement within the expected uncertainty. A second, independent, normalization method is under development, which is based on relative measurements versus the  $n$ - $p$  scattering cross section [10].

The data are compared with model predictions in Fig. 2, where the upper and lower panels show phenomenological (I–III,VII) and microscopic (IV–VI) models, respectively. Model I refers to a recent phenomenological global optical

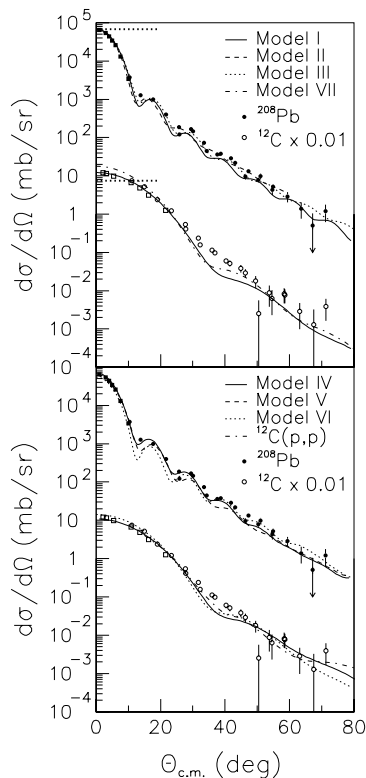


FIG. 2. Angular distributions of elastic neutron scattering from  $^{12}\text{C}$  (open circles) and  $^{208}\text{Pb}$  (solid) at 96 MeV incident neutron energy. The  $^{12}\text{C}$  data and calculations have been multiplied by 0.01. The data by Salmon at 96 MeV [5] are shown as squares. Upper panel: predictions by phenomenological models (I–III, VII). The thick dotted horizontal lines show Wick's limit for the two nuclei. Lower panel: predictions by microscopic models (IV–VI), and data on elastic proton scattering from  $^{12}\text{C}$  [23]. See the text for details.

model potential (OMP) [6], which is valid for incident nucleon energies between 1 keV and 200 MeV and masses from 24 to 209. It is based on a smooth functional form for the energy dependence of the potential depths, and on physically constrained geometry parameters. An extensive collection of experimental datasets for different types of observables was used to determine the parameters of this OMP.

We have performed a Dirac scattering calculation [11] (model II), which uses a global nucleon-nucleus intermediate energy Dirac phenomenological optical potential for  $^{208}\text{Pb}$  [12]. The potential contains scalar and vector terms, based upon the Walecka model [13], and includes isospin dependence through a relativistic generalization [14] of the Lane model [15]. The isospin dependence was determined by simultaneous least-squares adjustment with respect to measured proton elastic scattering and neutron total cross section observables. Symmetrized Saxon-Woods form factors are used, and the potential contains a total of 20 parameters to describe nucleon scattering by  $^{208}\text{Pb}$  in the energy range 95–300 MeV. An OMP calculation [16], based on a dispersive OMP approach treating nonlocality in a manner similar to that of Perey and Buck [17] for energy dependences, is presented as model III.

Model IV is a microscopic ( $g$ -folding) prescription for the

optical potentials [18], where a complete  $(0+2)\hbar\omega$  model of the structure of  $^{12}\text{C}$ , and a Skyrme Hartree-Fock model for  $^{208}\text{Pb}$ , have been used in the foldings. The predictions were obtained employing the effective (medium modified) nucleon-nucleon ( $NN$ ) interaction based upon the Bonn- $B$  interaction [19].

Model V is a Lane-consistent, semimicroscopic OMP [20], which is built by folding radial matter densities from a Hartree-Fock-Bogolyubov calculation (using the Gogny D1S effective interaction) with an OMP in nuclear matter that is based on an extension of that of Jeukenne, Lejeune, and Mahaux [21]. This extended OMP features strong renormalizations of its isovector components, and has recently been tested extensively against  $(p,p)$  and  $(n,n)$  data, as well as  $(p,n)$  IAS data [20].

Finally, the elastic observable was generated by a multiple-scattering expansion of the optical potential in terms of the free  $NN$  transition amplitude, calculated in the single-scattering  $t\rho$  approximation [22] (model VI). In the description of the target nucleus, there is no distinction between protons and neutrons. For  $^{12}\text{C}$ , the matter density distribution is deduced directly from the harmonic-oscillator shell model, with  $b=1.55$  fm. In the case of  $^{208}\text{Pb}$ , a two-parameter Fermi matter density distribution with halfway radius 6.62 fm and diffuseness 0.55 fm has been used.

When comparing these predictions with data, a few striking features are evident. First, all models are in reasonably good agreement with the  $^{208}\text{Pb}$  data. It should be pointed out that none of the predictions contain parameters adjusted to the present experiment. In fact, they were all made before data were available. Even the absolute scale seems to be under good control, which is remarkable, given that neutron beam intensities are notoriously difficult to establish. The level of agreement between models and data has been inspected by computing the  $\chi^2$ . For this exercise, only the uncertainties due to counting statistics have been used. Models III and IV have the lowest  $\chi^2$ , with models I and V in a second group. It should be pointed out, however, that the results are not dramatically different for the various models. That models III and IV are in best agreement is not surprising, because they are single-nucleus models, while models with a larger range of validity give a less perfect description for a particular nucleus. Model II was determined by simultaneously fitting a large proton data set and a small neutron data set (mostly total cross sections). For such a procedure, the agreement is surprisingly good.

A normalization error can produce a major  $\chi^2$  contribution. Therefore, we have tested to renormalize all theories to produce a minimum  $\chi^2$ . The absolute  $\chi^2$  values were reduced by this procedure, but the order between the models concerning the level of agreement was unchanged. What is notable is that models III and IV required very small renormalizations, 1–4%, with models I and V in a second group with renormalizations of about 14%.

Second, all models fail to describe the  $^{12}\text{C}$  data in the  $30^\circ$ – $50^\circ$  range. The models predict a saddle structure, which is not evident from the data. The reason for this mismatch might be that there are target correlations other than Pauli principle that are not included in the theoretical models.

It can be noted that proton scattering data on  $^{12}\text{C}$  at 95 MeV [23], which should agree with our data if isospin were a good symmetry, are closer to our data than the theory models are. The disagreement between models and  $^{12}\text{C}$  data should not be overemphasized though. Models which presume mean-field properties of nuclei to be dominant can have problems describing  $^{12}\text{C}$  data, because surface effects are very important in  $^{12}\text{C}$ .

The models above are all valid for spherical nuclei. It is known, however, that  $^{12}\text{C}$  to a significant degree displays properties of a three- $\alpha$  cluster. Coexistence of such a structure with a spherical shape might result in a matter distribution with a more diffuse edge than anticipated by the spherical models, and thus the predicted structure could be washed out.

We have developed a toy model to investigate this hypothesis. The increased effective radius of the  $^{12}\text{C}$  ground state due to three- $\alpha$  cluster effects has been studied theoretically for proton elastic scattering, however, at higher energies [24]. We have modified model I, using the parameters of Ref. [24], to calculate the elastic neutron scattering cross section (model VII). As can be seen in Fig. 2, this modification moves the prediction closer to the data in the  $30^\circ$ – $50^\circ$  range, but at the expense that the description gets worse at small angles. It should be pointed out, however, that this should only be seen as an indication of a possible cause of the effect, since the model is too simplified to allow quantitative conclusions.

A basic feature of the optical model is that it establishes a lower limit on the differential elastic scattering cross section at  $0^\circ$  if the total cross section is known, often referred to as Wick's limit. It has been observed in previous experiments at lower energies that for most nuclei, the  $0^\circ$  cross section falls

very close to the Wick's limit, although there is no *a priori* reason why the cross section cannot exceed the limit significantly. An interesting observation is that the present  $^{208}\text{Pb}$  data are in good agreement with the Wick's limit, while the  $^{12}\text{C}$   $0^\circ$  cross section lies about 70% above the limit. A similar behavior has previously been observed in neutron elastic scattering at 65 MeV [3], where the  $^{12}\text{C}$  data overshoot the Wick's limit by about 30%, while the  $^{208}\text{Pb}$  data agree with the limit. A follow-up experiment on the  $^{12}\text{C}$  cross section at  $0^\circ$  is under analysis.

In short, first results on elastic neutron scattering from  $^{12}\text{C}$  and  $^{208}\text{Pb}$  at 96 MeV incident neutron energy have been presented, and compared with theory predictions. This experiment represents the highest neutron energy where the ground state has been resolved from the first excited state in neutron scattering. The measured cross sections span more than four orders of magnitude. Thereby, the experiment has met—and surpassed—the design specifications. The overall agreement with theory model predictions, both phenomenological and microscopic, is good. In particular, the agreement in absolute cross section scale is impressive. A detailed account of all aspects of the measurements, including more detailed comparisons with theoretical models, is under preparation [25].

We wish to thank the technical staff of The Svedberg Laboratory for enthusiastic and skillful assistance. The computational aid of S. Y. van der Werf is gratefully acknowledged. This work was supported by the HINDAS project of the fifth EU framework program, as well as by Vattenfall AB, Swedish Nuclear Fuel and Waste Management Company, Swedish Nuclear Power Inspectorate, Barsebäck Power AB, Ringhals AB, Swedish Defense Research Agency, and the Swedish Research Council.

- 
- [1] A. Koning *et al.*, *J. Nucl. Sci. Technol.* **2**, 1161 (2002).  
 [2] See, e.g., *Neutron-Nucleus Collisions: A Probe of Nuclear Structure*, edited by J. Rapaport, R.W. Finlay, S.M. Grimes, and F.S. Dietrich, AIP Conf. Proc. No. 124 (AIP, New York, 1985).  
 [3] E.L. Hjort *et al.*, *Phys. Rev. C* **50**, 275 (1994).  
 [4] J. Klug *et al.*, *Nucl. Instrum. Methods Phys. Res. A* **489**, 282 (2002).  
 [5] G.L. Salmon, *Nucl. Phys.* **21**, 15 (1960).  
 [6] A.J. Koning and J.P. Delaroche, *Nucl. Phys.* (to be published).  
 [7] R.W. Finlay *et al.*, *Phys. Rev. C* **47**, 237 (1993).  
 [8] J. DeJuren and N. Knable, *Phys. Rev.* **77**, 606 (1950).  
 [9] R.G.P. Voss and R. Wilson, *Proc. R. Soc. London, Ser. A* **236**, 41 (1956).  
 [10] C. Johansson *et al.* (unpublished).  
 [11] R. Kozack and D.G. Madland, *Nucl. Phys.* **A509**, 664 (1990).  
 [12] R. Kozack and D.G. Madland, *Phys. Rev. C* **39**, 1461 (1989).  
 [13] B.D. Serot and J.D. Walecka, *Adv. Nucl. Phys.* **16**, 1 (1986).  
 [14] B.C. Clark, S. Hama, E. Sugarbaker, M.A. Franey, R.L. Mercer, L. Ray, G.W. Hoffman, and B.D. Serot, *Phys. Rev. C* **30**, 314 (1984).  
 [15] A.M. Lane, *Nucl. Phys.* **35**, 676 (1962).  
 [16] P. Romain and J.P. Delaroche, in *Proceedings of a Specialists Meeting*, edited by O. Borsillon, J.P. Delaroche, A. Koning, and P. Nagel (OECD, Paris, 1997), p. 167.  
 [17] F. Perey and B. Buck, *Nucl. Phys.* **32**, 353 (1962).  
 [18] K. Amos, P.J. Dortmans, H.V. von Geramb, S. Karataglidis, and J. Raynal, *Adv. Nucl. Phys.* **25**, 275 (2000).  
 [19] R. Machleidt, *Adv. Nucl. Phys.* **19**, 189 (1989).  
 [20] E. Bauge, J.P. Delaroche, and M. Girod, *Phys. Rev. C* **63**, 024607 (2001).  
 [21] J.P. Jeukenne, A. Lejeune, and C. Mahaux, *Phys. Rev. C* **16**, 80 (1977).  
 [22] R. Crespo, R.C. Johnson, and J.A. Tostevin, *Phys. Rev. C* **46**, 279 (1992).  
 [23] G. Gerstein, J. Niederer, and K. Strauch, *Phys. Rev.* **108**, 427 (1957).  
 [24] J. Matero, *Z. Phys. A* **351**, 29 (1995).  
 [25] J. Klug *et al.* (unpublished).